

An algorithm to determine the slope of the spectral absorption of colored dissolved organic matter (CDOM) and detritus

Suresh, T.¹; Dias, A.B.¹; Desa, E.J.A.²; Sahay, A.³

¹ Marine Instrumentation Division, CSIR-National Institute of Oceanography, Goa, India, sureshnio@gmail.com, albertina.dias8@gmail.com

² Goa University, Goa 403004, India, erwindesa@gmail.com

³ Space Application Centre, Ahmedabad, India, arvindsahay@sac.isro.gov.in

Abstract

A simple method to determine the slope of the spectral variations of the combined absorption of the colored dissolved organic matter (CDOM) and detritus (CDM) is presented. This method uses the slope of the total absorption spectrum excluding the contribution of waters in lieu of the slope for the CDM. The errors in slopes using the new method decreased with the increase in the contributions of CDM to the total absorption. The relative errors were less than 10% when the CDM contributions were above 60% and even at very low contributions of CDM of 25%, the errors in the slopes were less than 40%. For estuarine and coastal waters rich in CDM, the errors in the slopes for CDM were less than 10% using this simple method. The absorption of CDM derived using the slope with the new method in a semi-analytical algorithm QAAV6 showed improved performance with RMSE of 0.07, 0.0119 and 0.0027 at 405, 555 and 665 nm respectively and with $R^2 > 0.95$ at all spectral range. The method provided values of the spectral absorption due to CDM with fewer errors when validated with the satellite derived data from MODIS and SeaWiFS. This method to determine the slope of CDM could be easily implemented in any model, as it was very generic in nature, simple, did not involve any mathematical model and avoid empirical methods. Since the method is also independent of any specific bands, it can be used for most ocean color satellites. Considering the performance of this new method and applicability for most water types, it was considered as a better option to derive the slope of CDM than using a constant value or deriving the slope with empirical method.

Keywords: CDOM, detritus; absorption, algorithm, CDM

A. Introduction

The inherent optical property of absorption is additive and the total absorption coefficient of water is given as the sum total of the absorption coefficients of the partitioned components, as given in equation 1 (Mobley 1994).

$$a(\lambda) = a_w(\lambda) + a_{ph}(\lambda) + a_g(\lambda) + a_d(\lambda) \quad (1)$$

Here $a_w(\lambda)$ is the absorption coefficient due to pure water and the contributions of other optically active constituents are $a_{ph}(\lambda)$ due to phytoplankton pigments, $a_g(\lambda)$ for chromophoric or colored dissolved matter (CDOM) and $a_d(\lambda)$ due to non-algal particles (NAP) or detritus. Presently there are semi-analytical and empirical algorithms that derive the inherent optical properties (IOPs) of water also known as IOP inversion algorithms for remote sensing applications with the apparent optical property of remote sensing reflectance as input (IOCCG, 2006). CDOM exhibits a simple pattern of spectral variation, exponentially decaying with increasing wavelength (Jerlov, 1976). It has been observed that absorption of non-algal particles (NAP) or detritus too show a similar pattern of spectral variations (Bricaud et al., 1981; Roesler et al., 1989). Hence the spectral variations of the CDOM, detritus and the combined CDOM + detritus follow the pattern of the exponential decay with an increase in wavelength and are generally given by the equation 2. Here $x=g$ for CDOM and $x=d$ for detritus and $x=dg$ for CDOM + detritus.

$$a_x(\lambda) = a_x(\lambda_0) e^{-S_x(\lambda-\lambda_0)} \quad (2)$$

Where $a_x(\lambda)$ is the spectral absorption coefficient (m^{-1}), $a_x(\lambda_0)$ is the absorption coefficient (m^{-1}) at a reference wavelength, λ_0 (nm) and S_x is the slope (nm^{-1}). The slope is found by a linear fit of the log transformed $a_x(\lambda)$ over a spectral range. The $a_x(\lambda_0)$ is usually considered as a representative of the concentration and the slope of CDOM provide information about its source. This slope also varies with the spectral range (Twardowski et al. 2004). The reference wavelength λ_0 is usually selected from the lower wavelength of UV or blue region and for remote sensing applications; it is usually 412 or 443 nm. Thus, the two variables that define the spectral absorptions of CDOM, detritus or CDOM + detritus are their absorption at λ_0 and slope S_x .

The four components model given in equation 1 is reduced to three components with combination of $a_g(\lambda) + a_d(\lambda) = a_{dg}(\lambda)$. This alliance has been for convenience and it helped in the developments of optical inversion algorithms with fewer parameters to derive and reduce the errors. The light properties of both CDOM and NAP differ, as NAP can scatter light while CDOM only absorbs and do not scatter. The merger of CDOM and NAP is also known as colored detrital material, CDM =

CDOM + NAP (Siegel, 2002). For the open ocean and case 1 water CDOM and NAP were reported to covary well with phytoplankton (Morel and Prieur 1977). In the open ocean, the contribution of CDOM and detritus could be negligible which however may not be the scenario in coastal and estuarine waters.

The slope of CDM, S_{dg} was often taken as constant in most models with low values of S_{dg} for open ocean or case 1 waters and relatively higher values for other waters. The typical values of S_{dg} which were representative of the water or generic and considered for the algorithm were 0.0206 for GSM model (Garver and Siegel 1997; Maritorena et al., 2002), 0.015 for QAA (Lee et al., 2002), 0.0225 for MODIS semi-analytical algorithm (Carder et al. 1999, 2004), 0.014 for semi-analytical model by Sathyendranath and Platt (1997, 1998, 2001) and 0.018 for the constrained linear matrix inversion method (Hoge and Lyon 1996). However, some models derived S_{dg} using empirical relations within the defined boundaries such as the updated QAA version 5 and 6 (<http://ioccg.org/resources/software/>).

It was observed that the spectral shape of the $a_{dg}(\lambda)$ and $a_t(\lambda)$, where $a_t(\lambda) = a(\lambda) - a_w(\lambda)$, had similar spectral variations for the measured data of Goa and this information of similarity in shape of spectral variations of $a_t(\lambda)$ and $a_{dg}(\lambda)$ formed the basis for the development of a simple algorithm to determine S_{dg} . The objective of this study was to derive S_{dg} exploiting a simple similarity in shape property of $a(\lambda) - a_w(\lambda)$ and $a_{dg}(\lambda)$, show its application, validate and evaluate its performance by applying this method in an available semi-analytical model and also compare with the $a_{dg}(\lambda)$ derived from the ocean color satellite data.

In the next section, the rationale and the condition for the applicability of this simple method to derive S_{dg} is established. Thereafter S_{dg} obtained with this method was compared with S_{dg} derived from a semi-analytical model and the suitability of this new method for remote sensing application was demonstrated, validating measured $a_{dg}(\lambda)$ with those derived from the satellite data.

B. Method

The data used were, the optical data measured in the coastal and estuarine waters of Goa, India, a region on the west coast of India, the NOMAD data (Werdell and Bailey 2005) and the satellite derived data from SeaBASS (Bailey and Werdell 2006). The measurements were carried out in the coastal waters and in both Mandovi and Zuari estuaries (15.43- 15.48° N latitude and 73.6 – 74.05° E longitude) during March 2014 – May 2016. Total CDOM data records used were 364. The measured data for the Goa were the absorption due to CDOM, detritus, and phytoplankton measured from the water samples collected at discrete depths from various stations of the coastal waters and two

estuaries, Mandovi and Zuari of Goa. These measurements were carried out with a double-beam spectrophotometer (Shimadzu, UV2600), following the standard protocol (Mitchell et al. 2003). NOMAD: the NASA bio-Optical Marine Algorithm Data set Version 2.0 ALPHA, created on 18 July 2008, was the publicly available high quality in-situ bio-optical data measured from various waters over the globe and have been used often for the ocean color algorithm developments and also satellite data product validations. (http://seabass.gsfc.nasa.gov/wiki_files/NOMAD/files/nomad_seabass_v2.a_2008200.txt). All the NOMAD data were used for this study. The satellite validation data included the in-situ measured data measured from various global waters and the satellite derived optical parameters using various algorithms from the co-located locations. The SeaBASS data available was last updated on 2016-10-05 and the data for SeaWiFS, MODIS Aqua and Terra were downloaded for this study on 31 October 2016 from <http://seabass.gsfc.nasa.gov/search>.

The slope was determined by the log-transformed spectral absorption in the spectral range of 400-650 nm with the linear least-square fitting model. The slopes of CDOM+ detritus, S_{dg} and the slopes of the spectral $a_t(\lambda)$, S_{at} were compared for the waters of Goa and NOMAD data and they showed close match for both the data (Fig.1) with R^2 , slope, and intercept of the fit of 0.73 , 0.82, 0.003 respectively for NOMAD data and 0.84, 0.7 and 0.004 respectively for the waters of Goa. The close match of S_{dg} with S_{at} affirmed the reasons to accept S_{at} in lieu of S_{dg} . Next, the conditions for its validity were examined.

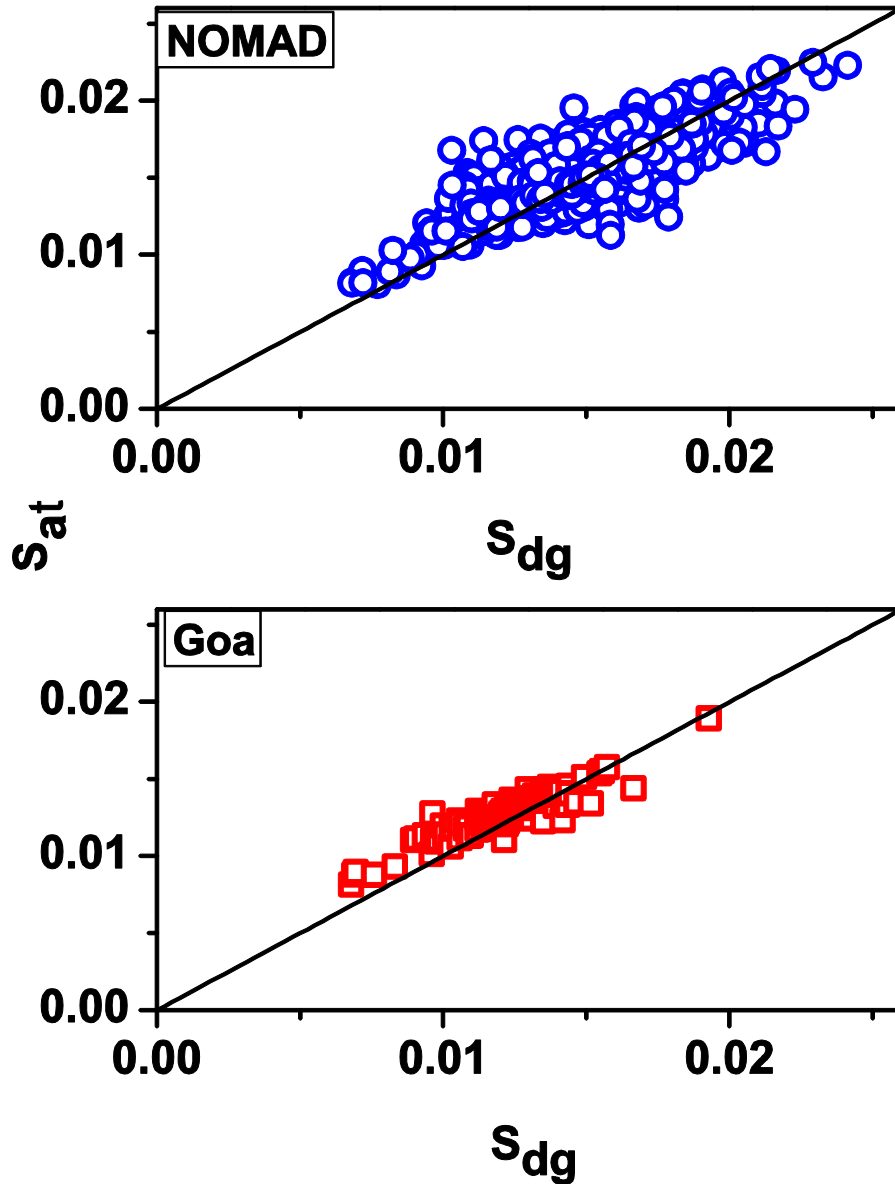


Fig.1 .Variations of S_{at} and S_{dg} showing high correlation between them indicated by 1:1 line. The data used were from NOMAD (top) and the waters of Goa (bottom)

Since total absorption is the sum total of the absorption of each component (see equation 1), the $a_t(\lambda)$ will be closer to $a_{dg}(\lambda)$ if $a_{ph}(\lambda)$ is relatively low. Hence the spectral shape of $a_t(\lambda)$ will mimic $a_{dg}(\lambda)$ under situations when the absorption of CDM is relatively higher than the absorption due to phytoplankton. The errors in S_{dg} by equating S_{at} to S_{dg} will depend on the how close the $a_t(\lambda)$ is to $a_{dg}(\lambda)$. Three data sets, from the coastal and estuarine waters of Goa, NOMAD and the synthesized optical data of IOCCG (<http://ioccg.org/resources/data/>) were used to study these errors. In all the three data sets the errors decreased as $a_{dg}(\lambda)/a_t(\lambda)$ ratio increased and the errors were minimum when $a_{dg}(\lambda)/a_t(\lambda)$ approached closer to unity (Fig. 2). Since the coastal and estuarine waters of Goa were rich in CDM and $a_{dg}(\lambda)/a_t(\lambda)$ values were close to 1, the S_{at} compared well with the S_{dg} . NOMAD

data were from various water types and the ratio $a_{dg}(\lambda)/a_t(\lambda)$ varied from 0.1 to 0.93 and for the synthesized data of IOCCG, the ratio varied from 0.26 to 0.85. In all cases, the relative percentage errors in S_{at} with respect to S_{dg} were mostly limited to a maximum of 40%. The relative percent error is given in equation 6. For absorption ratio $a_{dg}(\lambda)/a_t(\lambda) > 0.6$ the errors were less than 10% and hence the new method to use S_{at} in lieu of S_{dg} was self-evident for such data types available from the coastal and estuarine waters.

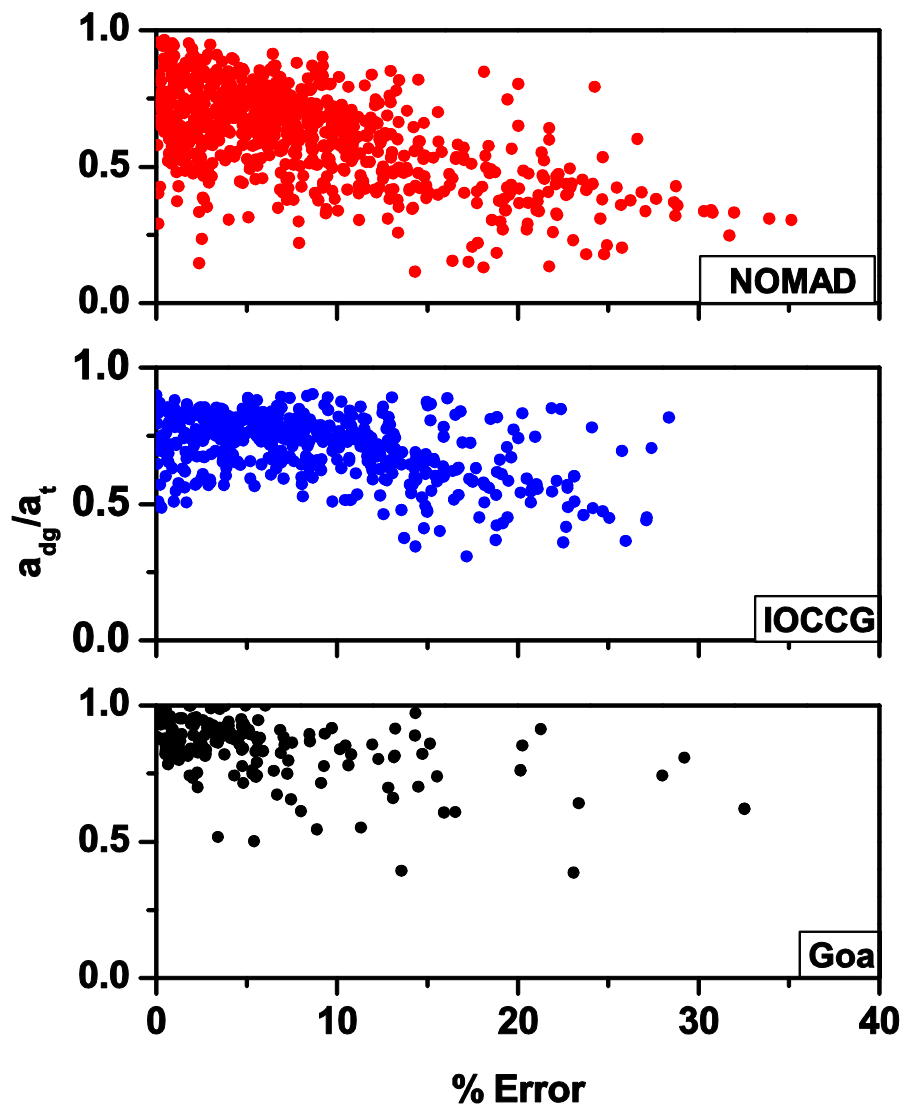


Fig.2. Variations of the contributions of CDM to the total absorption of water, a_{dg}/a_t at 532 nm and the % error in the slope S_{at} compared to S_{dg}

Having confirmed and verified the assumption of S_{at} and S_{dg} being comparable for most water types within an upper limit of 40% error, the S_{at} was applied in lieu of S_{dg} in a semi-analytical algorithm to derive IOPs. The latest available version of QAA V6 updated in 2015 was used to test the new method (http://www.ioccg.org/groups/Software_OCA/QAA_v6_2014209.pdf). The QAAV6 was

tweaked and the new method was used to determine S_{dg} . NOMAD data was used for testing the new method in QAAV6 and the original QAAV6. The modified flow of the QAAV6 algorithm that used this similarity property of S_{at} is given in Fig. 3. The quasi semi-analytical algorithm QAAV6 used remote sensing reflectance $R_{rs}(\lambda)$ from NOMAD data and derived the $a_t(\lambda)$ (Step 6) as in Fig. 3. The slope S_{at} was derived using $a_t(\lambda)$. This S_{at} was used in lieu of S_{dg} to derive $a_{dg}(\lambda)$. All other parameters and the semi-analytical and empirical methods used in QAAV6 remained the same without any change. The S_{dg} in the earlier version of QAA used a constant value of 0.015, while in later versions S_{dg} was derived using an empirical relation based on the ratio of remote sensing reflectance at 443 and 555 nm. The $a_{dg}(\lambda)$ was derived using QAAV6 and compared with the modified method using S_{at} .

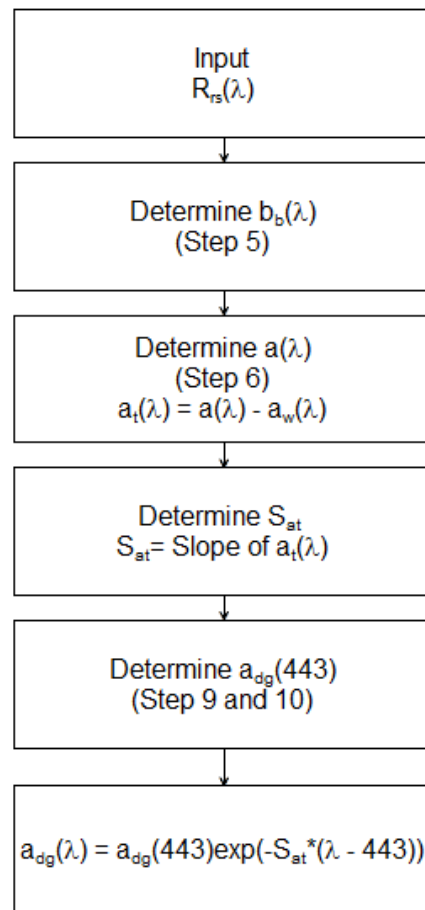


Fig.3 Determining the spectral $a_{dg}(\lambda)$ as in QAAV6, using the slope S_{at} in lieu of S_{dg}

This method was also applied to the satellite data. The SeaBASS data used for the validations of satellites was used for this study. The in-situ measured data and co-located satellite derived products a_{giop} and adg_{giop} derived using an inversion model were downloaded for the satellites, SeaWiFS, MODIS Terra and MODIS Aqua from the SeaBASS site. The method as given in Fig. 3 was

adopted, with $a_t(\lambda)$ obtained from $a\text{-giop}(\lambda)$ of each satellite data and then the slope S_{at} of $a_t(\lambda)$ was determined. The $a_{dg}(\lambda_0)$ was the $a_{dg}(\lambda)$ at the lowest band of the $adg\text{-giop}(\lambda)$, which was 412 nm. The in-situ measured $a_{dg}(\lambda)$ of the respective satellite data were then compared with the satellite derived $adg\text{-giop}(\lambda)$.

C. Results

The error analyses were carried out with statistical parameters such as bias, RMSE (root mean square error), the coefficient of determination R^2 , regression between the model and the measured. a_{dg_Model} refers to $a_{dg}(\lambda)$ derived using the model and $a_{dg_Measured}$ refers to $a_{dg}(\lambda)$ measured from the waters samples.

$$Bias = \frac{1}{n} \sum_1^n (a_{dg_Model} - a_{dg_Measured}) \quad (3)$$

$$RMSE = \sqrt{\frac{1}{n-2} \sum_1^n (a_{dg_Model} - a_{dg_Measured})^2} \quad (4)$$

$$a_{dg_Measured} = m(a_{dg_Model}) + c \quad (5)$$

$$Error = 100 \frac{S_{at} - S_{dg}}{S_{dg}} \quad (6)$$

1) NOMAD data

The S_{dg} derived using the NOMAD data varied from 0.0023 to 0.024. The S_{at} using $a_t(\lambda)$ derived from QAAV6 compared well than S_{dg} obtained from the empirical relation in QAA V6 (Fig. 4). The S_{dg} derived using empirical method varied within a narrow range 0.01 to 0.017, maintaining almost a constant value over a wide range of S_{dg} from NOMAD data, while S_{at} maintained a wider variability of 0.0014 to 0.03 and correlated better with S_{dg} calculated with NOMAD $a_{dg}(\lambda)$. For S_{dg} values less than zero obtained using QAAV6, the lower limit was set to 0.01.

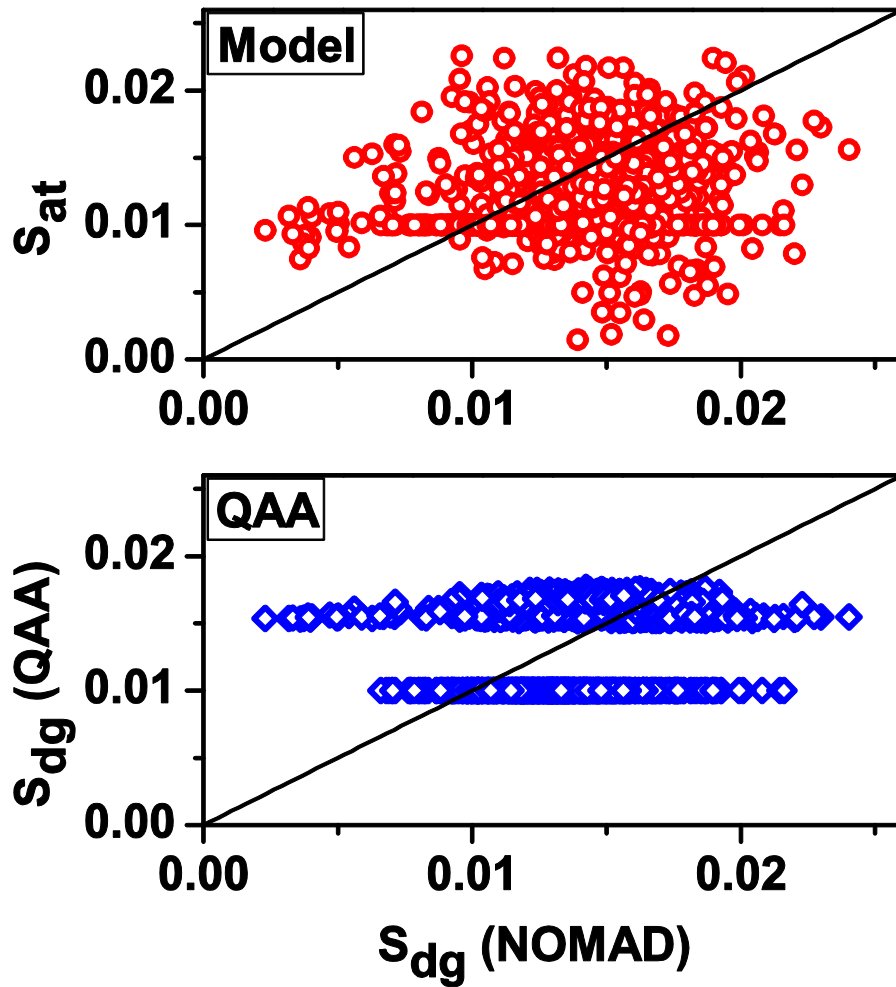


Fig.4 Comparisons of S_{at} using $a_t(\lambda)$ and S_{dg} derived using empirical relations in QAAV6 with S_{dg} of the measured NOMAD data

The tweaked QAAV6 with the new method performed relatively better with higher R^2 (> 0.95) at all wavelengths, lower RMSE and regression slope close to 1 and very low intercept as compared to QAAV6 (Fig. 5).

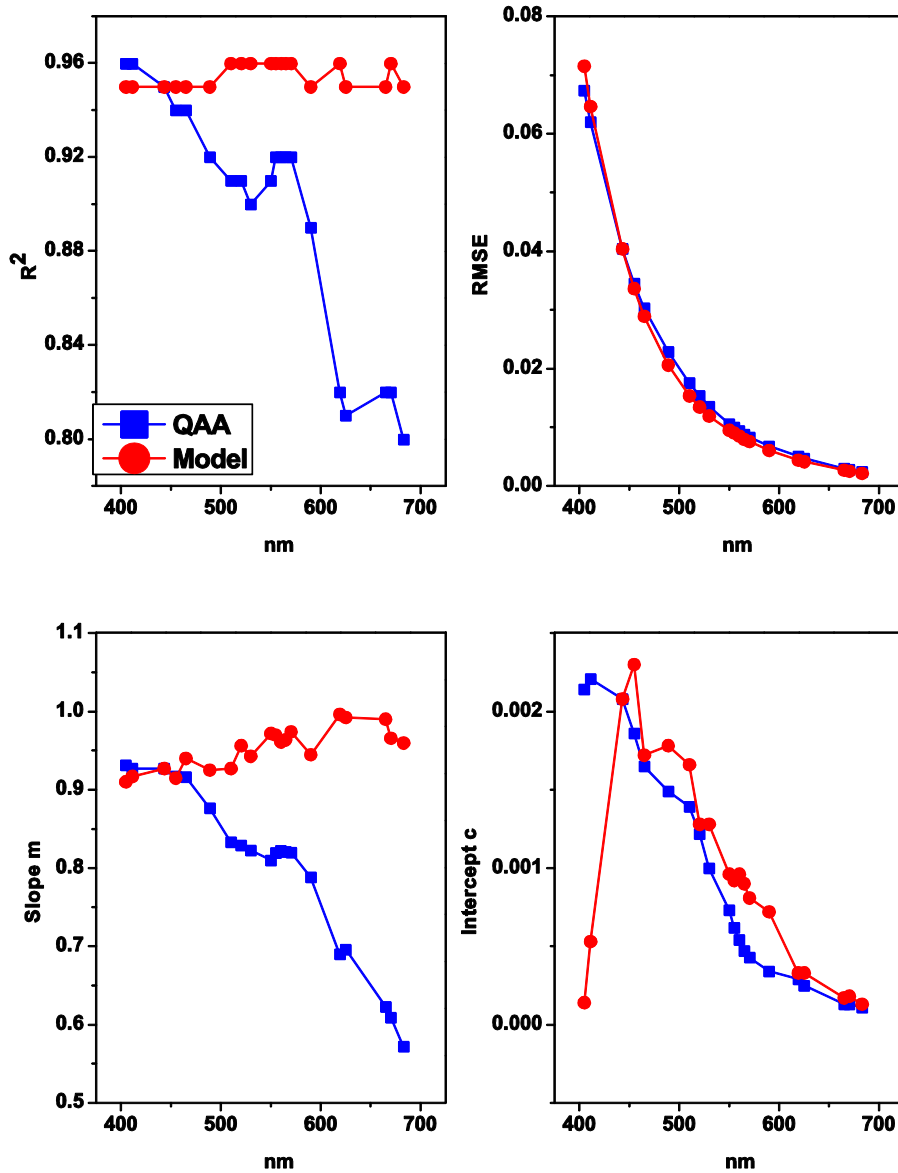


Fig.5 Error statistics to indicate the performance of the QAAV6 with S_{at} (Model) and the original QAAV6 (QAA) indicated by the R^2 (top left), RMSE (top right), slope m (bottom left) and the intercept c (bottom right)

2) Satellite data

The satellite validation data from the SeaBASS site had the measured data and the satellite derived products of the co-located locations. The satellite products of absorptions of waters with its components which included total, CDM and phytoplankton absorptions were derived using GIOP algorithm. The $a_{dg}(\lambda)$ derived using the method described here compared better than those derived using the inversion model from the satellite data of SeaWiFS, MODIS Terra and MODIS Aqua with better scores of error statistics for all bands, such as higher R^2 , lower RMSE (Fig. 6). Here all the

data were used for comparisons without discarding any outliers. There were enhanced improvements observed using the new method by discarding few outliers, as compared to the same satellite derived $a_{dg}(\lambda)$. The RMSE at 443 were 0.163, 0.119, 0.16 for SeaWiFS, MODIS Terra and MODIS Aqua respectively.

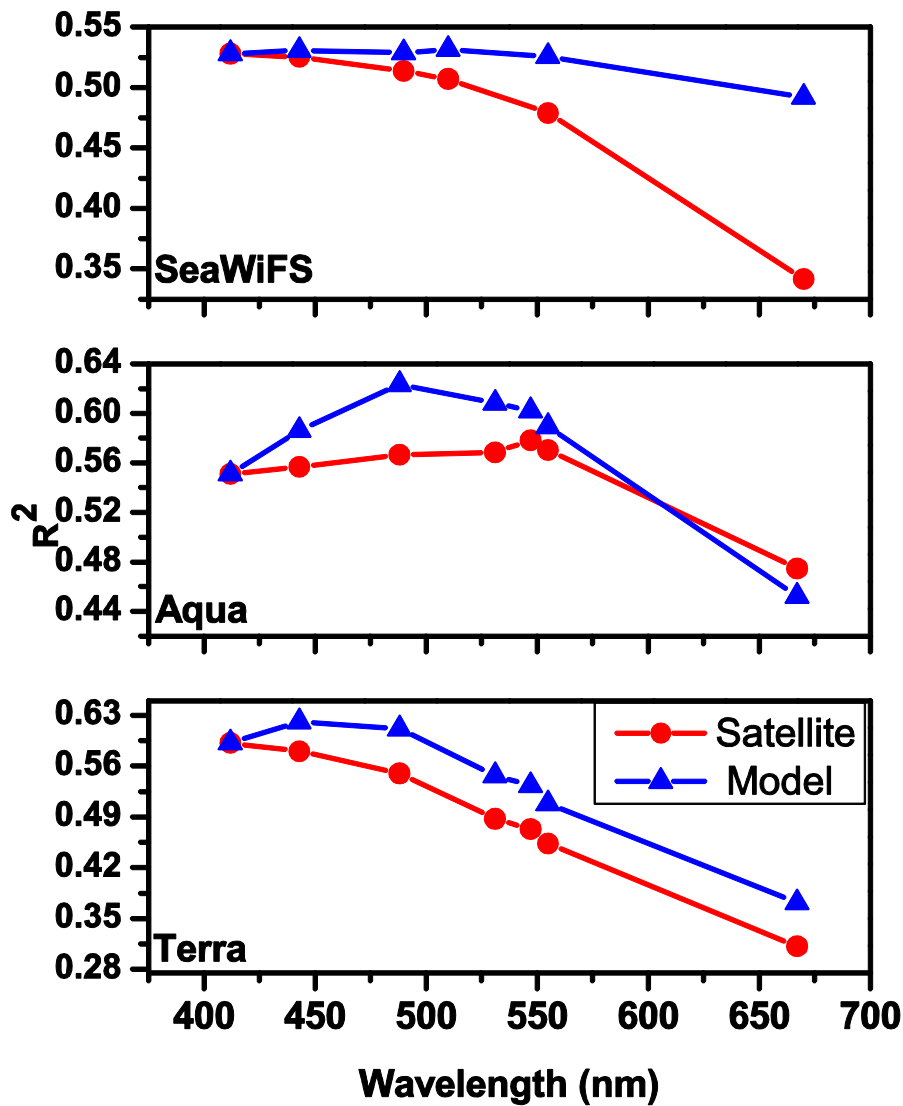


Fig.6 The coefficient of determination R^2 for the comparison of the $a_{dg}(\lambda)$ with the measured, new method (indicated as Model) and those derived from using the original inversion method in satellite data processing (Satellite)

D. Discussion

The new method to use S_{at} in lieu of S_{dg} was found as a good option for waters with high CDOM and detritus. When the contributions of CDM to the total absorption (excluding absorption by water) were above 60%, the errors were limited only to 10%. These errors too decreased as the contribution of both CDOM and detritus increased (Fig. 2). Though this method was better suited for waters rich

in CDOM and detritus as compared to phytoplankton, considering CDOM from various water types and with the contributions of CDM varying from a lower limit of 25%, the maximum errors observed between S_{at} and S_{dg} were less than 40%.

The $a_{dg}(\lambda)$ derived showed better performance after implementing the new method in the semi-analytical model, QAAV6 than deriving $a_{dg}(\lambda)$ from the original QAAV6 method. The new method when applied to the IOPs from the satellite data of Terra, Aqua and SeaWiFS could derive spectral $a_{dg}(\lambda)$ with better accuracy. The performance of the same IOP inversion algorithms to derive $a_{dg}(\lambda)$ from satellite data have been observed to vary with satellite sensors (Naik et al. 2010) and similarly here too the performance of MODIS was better than that of SeaWiFS.

This method to determine the slope, S_{dg} could be easily implemented in any model, as it was very generic in nature, simple, did not involve any mathematical model and avoid empirical methods. Since the method is also independent of any specific bands, it can be used for most ocean color satellites.

Since the spectral model given by equation 2 requires only two parameters, the slope S_{dg} and $a_{dg}(\lambda_o)$, the model accuracy to derive $a_{dg}(\lambda_o)$ will depend on two parameters, $a_t(\lambda)$ the total spectral absorption and the $a_{dg}(\lambda_o)$, the CDM at a reference wavelength. The accuracy of $a_t(\lambda)$ is not important; rather its spectral variation does matter, as the slope must match the slope of the spectral variations of $a_{dg}(\lambda)$. There should be sufficient values of $a_t(\lambda)$ at wavelengths spaced apart from blue towards red, that will allow modelling the $a_t(\lambda)$ with better accuracy as given in equation 2. However, apart from the slope of $a_t(\lambda)$, the $a_{dg}(\lambda)$ can only be determined with better accuracy if $a_{dg}(\lambda_o)$ is available with minimum error.

Though the $a_{dg}(\lambda)$ can be determined with, better accuracy there is no assurance of having any improvements in the accuracy of the $a_{ph}(\lambda)$. This will solely depend on the method used to derive $a_{ph}(\lambda)$. If it is obtained as a remnant of the $a_{dg}(\lambda)$ from $a_t(\lambda)$ i.e. $a_{ph}(\lambda) = a_t(\lambda) - a_{dg}(\lambda)$, the accuracy of $a_{ph}(\lambda)$ will depend on both, $a_t(\lambda)$ and $a_{dg}(\lambda)$. Hence with a method to derive $a_t(\lambda)$ with better accuracy over the spectral range from blue to red such as Suresh et al., 2016 or others and a good empirical algorithm to derive CDM at a reference $a_{dg}(\lambda_o)$, $a_{ph}(\lambda)$ could be obtained with much improved accuracy by applying this method.

E. Conclusions

The new method to use S_{at} in lieu of S_{dg} was found as a good option for waters with high CDOM and detritus absorption compared to phytoplankton. The relative errors in S_{at} compared with S_{dg} decreased as the contribution of both CDOM and detritus increased. When the contributions of CDM

to the total absorption (excluding absorption by water) were above 60%, the errors between S_{at} and S_{dg} were limited only to 10 %. Though this method was suited for waters rich in CDOM and detritus as compared to phytoplankton, even with the contributions of CDM varying from a lower limit of 25%, the maximum errors observed between S_{at} and S_{dg} were less than 40%. The simple method to derive the slope of $a_{dg}(\lambda)$, using the similarity in the shapes of spectral variations of $a_t(\lambda)$ and $a_{dg}(\lambda)$ was found to be a better option than assuming a constant value of S_{dg} , or using empirical relation to derive S_{dg} . S_{dg} cannot be taken as a constant as it varies with water types and the sources of CDOM.

This was a simple method to derive S_{dg} that could be used with most available IOP models as it is generic in nature, independent of the bands, does not use any mathematical model or empirical relations. The $a_{dg}(\lambda)$ derived using this new method performed better when compared to the empirical relation used in the semi-analytical algorithm. The accuracy of the $a_{dg}(\lambda)$ derived from the satellite data of SeaWiFS, MODIS Aqua, and Terra improved when this method was applied to the IOPs derived from the satellite data.

References

1. Bailey, S.W., & Werdell, P.J. (2006). A multi-sensor approach for the on-orbit validation of ocean color satellite data products. *Remote Sensing Environment*, 102, 12-23.
2. Bricaud, A., Morel, A., & Prieur, L. (1981). Absorption by Dissolved Organic Matter of the Sea (Yellow Substance) in the UV and Visible Domains. *Limnology and Oceanography*, 26(1), 43-53.
3. Carder, K. L., Chen, F. R., Cannizzaro, J. P., Campbell, J. W. & Mitchell, B. G. (2004). Performance of the MODIS semi-analytical ocean color algorithm for chlorophyll-a. *Advances in Space Research*, 33(7), 1152-1159.
4. Carder, K.L., Chen, F.R., Lee, Z.P., Hawes, S.K. & Kamykowski, D. (1999). Semianalytic moderate-resolution imaging spectrometer algorithms for chlorophyll a and absorption with bio-optical domains based on nitrate-depletion temperatures. *Journal of Geophysical Research-Oceans*, 104, 5403-5421.
5. Garver, S.A. & Siegel, D.A. (1997). Inherent Optical Property Inversion of Ocean Color Spectra and Its Biogeochemical Interpretation, Time Series from the Sargasso Sea. *Journal of Geophysical Research, Oceans*, 102 (C8), 18607-18625.
6. Hoge, F. E. & Lyon, P. E. (1996). Satellite retrieval of inherent optical properties by linear matrix inversion of oceanic radiance models: An analysis of model and radiance measurement errors. *Journal of Geophysical Research-Oceans*, 101, 16631-16648.
7. <http://seabass.gsfc.nasa.gov/wiki/NOMAD>
8. http://www.ioccg.org/groups/Software_OCA/QAA_v6_2014209.pdf
9. Jerlov, N. G. (1976). *Optical oceanography*. New York, Elsevier.
10. Lee, Z.P. (2006). *Remote Sensing of Inherent Optical Properties: Fundamentals, Tests of Algorithms, and Applications*. Reports of the International Ocean Colour Coordinating Group. Dartmouth, Canada, IOCCG.
11. Lee, Z.P., Carder, K. L., & Arnone, R. A. (2002). Deriving Inherent Optical Properties from Water Color: A Multiband Quasi-Analytical Algorithm for Optically Deep Waters. *Applied Optics*, 41 (27), 5755-5772.

12. Loisel, H., Vantrepotte, V., Dessailly, D. & Mériaux, X. (2014). Assessment of the Colored Dissolved Organic Matter in Coastal Waters from Ocean Color Remote Sensing. *Optics Express*, 22 (11), 13109-13124.
13. Maritorena, S., Siegel, D. & Peterson, A.R. (2002). Optimization of a Semianalytical Ocean Color Model for Global-Scale Applications. *Applied Optics*, 41 (15), 2705-2714.
14. Mitchell, B.G., Kahru, M., Wieland, J., & Stramska, M. (2003). Determination of spectral absorption coefficients of particles, dissolved material and phytoplankton for discrete water samples, In Mueller, J.L., Fargion, G.S. and McClain, C.R., (Eds), *Ocean Optics Protocols for Satellite Ocean Color Sensor Validation* (pp39-64), NASA/TM-2003-211621/Rev4-Vol.IV.
15. Mobley, C. D. (1994). *Light and Water; Radiative Transfer in Natural Waters*, Academic Press, San Diego, 592 p
16. Morel, A., & Prieur, L. (1977). Analysis of variations in ocean color. *Limnology and Oceanography*, 22, 709-722.
17. Naik, P., Eurico J D'Sa, Goes, J.I., & Gomes, H.R. (2010). Assessment of Particulate Absorption Properties in the South eastern Bering Sea from in-Situ and Remote Sensing Data. *Journal of Applied Remote Sensing*, 4, 43520-43561.
18. Roesler, C. S., & Perry, M.J. (1995). In situ phytoplankton absorption, fluorescence emission, and particulate backscattering spectra determined from reflectance. *Journal of Geophysical Research: Oceans*, 100(C7), 13279-13294.
19. Roesler, C. S., Perry, M. J., & Carder, K. L. (1989). Modeling in situ phytoplankton absorption from total absorption spectra in productive inland marine waters. *Limnology and Oceanography*, 34, 1510-1523.
20. Sathyendranath, S. & Platt, T. (1998). Ocean-color model incorporating trans spectral processes. *Applied Optics*, 37(12), 2216-2227.
21. Sathyendranath, S., & Platt, T. (1997). Analytic model of ocean color. *Applied Optics*, 36, 2620-2629.
22. Sathyendranath, S., Cota, G., Stuart, V., Maass, H., & Platt, T. (2001). Remote sensing of phytoplankton pigments: a comparison of empirical and theoretical approaches. *International Journal of Remote Sensing*, 22 (2-3), 249-273.
23. Shanmugam, P. (2011). New Models for Retrieving and Partitioning the Colored Dissolved Organic Matter in the Global Ocean: Implications for Remote Sensing. *Remote Sensing of Environment*, 115 (6), 1501-1521.
24. Siegel, D. A. (2002). Global Distribution and Dynamics of Colored Dissolved and Detrital Organic Materials. *Journal of Geophysical Research*, 107 (C12), 3228.
25. Suresh, T., Talaulikar, M., Desa, J.A.E. & Lotlikar, A. (2016). Preliminary Results of an Algorithm to Determine the Total Absorption Coefficient of Water Proceeding SPIE, 9878, 98780E.
26. Twardowski, M. S., Boss, E., Sullivan, J.M., Percy, L., & Donaghay. (2004). Modeling the Spectral Shape of Absorption by Chromophoric Dissolved Organic Matter. *Marine Chemistry*, 89 (1-4), 69-88.
27. Wang, P., Boss, E., & Roesler, C. (2005). Uncertainties of Inherent Optical Properties obtained from Semi- Analytical Inversions of Ocean Color. *Applied Optics*, 44(19), 4074- 4085.
28. Werdell, P., J., & Bailey, S.W. (2005). An Improved in-Situ Bio-Optical Data Set for Ocean Color Algorithm Development and Satellite Data Product Validation. *Remote Sensing of Environment*, 98 (1), 122-140.